



HAL
open science

Tidally synchronized solar dynamo: a rebuttal

Henri-Claude Nataf

► **To cite this version:**

Henri-Claude Nataf. Tidally synchronized solar dynamo: a rebuttal. Solar Physics, 2022, 297, pp.107. 10.1007/s11207-022-02038-w . hal-03590783v2

HAL Id: hal-03590783

<https://hal.science/hal-03590783v2>

Submitted on 28 Jun 2022

HAL is a multi-disciplinary open access archive for the deposit and dissemination of scientific research documents, whether they are published or not. The documents may come from teaching and research institutions in France or abroad, or from public or private research centers.

L'archive ouverte pluridisciplinaire **HAL**, est destinée au dépôt et à la diffusion de documents scientifiques de niveau recherche, publiés ou non, émanant des établissements d'enseignement et de recherche français ou étrangers, des laboratoires publics ou privés.

Tidally synchronized solar dynamo: a rebuttal

Henri-Claude Nataf¹●●

© Springer ●●●●

Abstract The idea of a planetary origin for the solar cycle dates back to the nineteenth century. Despite unsurmounted problems, it is still advocated by some. Stefani, Giesecke, and Weier (2019) thus recently proposed a scenario based on this idea. A key argument they put forward is evidence that the ~ 11 years-solar cycle is *clocked*. Their demonstration rests upon the computation of a ratio proposed by Dicke (1978) applied to the solar cycle time series of Schöve (1955). I show that their demonstration is invalid, because the assumptions used by Schöve to build his time series force a *clocked* behaviour. I also show that instabilities in a magnetized fluid can produce fluctuation time series that are close to being *clocked*.

Keywords: Solar Cycle, Models; Solar Cycle, Observations

1. Introduction

The recent opening and publication by Courtillot, Le Mouél and Lopes (Malburet, 2019) of a *pli cacheté* (sealed letter), entrusted to the French Academy of Science by Jean Malburet in 1918 (Malburet, 1918), highlights the early interest in the search for a link between solar cycles and tides. In fact, the work of Malburet was already known from a detailed and luminous report he wrote (in french) for the journal '*L'Astronomie*' in 1925 (Malburet, 1925)¹. In that report, he correctly estimates the tidal forcing of planets on the Sun as being proportional to m_p/d_p^3 where m_p and d_p are the mass of a planet, and its distance from the Sun, respectively. This scaling yields tidal forcings proportional to ~ 4.0 , ~ 3.8 , ~ 1.8 , and ~ 1.7 , for Jupiter, Venus, Earth and Mercury, respectively (the contributions of the other planets are at least 10 times smaller). With this in mind, Malburet shows a good correspondance between the dates of solar

H.-C. Nataf
henri-claude.nataf@univ-grenoble-alpes.fr

¹ Univ Grenobles Alpes, CNRS, ISTERre, Grenoble, France.

¹This article is available on line from the Bibliothèque de France via Gallica: <https://gallica.bnf.fr/ark:/12148/bpt6k9628963x/f369.item>.

maxima and the dates of ‘weak deviations from Jupiter-Venus-Earth syzygies²’. Malburet’s idea was later taken up and extended by Wood (1972) and Okhlopkov (2016).

There are however two serious problems with this idea:

1. The amplitude of the tidal forcing on the Sun is extremely small ($< 10^{-8}$ kg m⁻³), yielding accelerations one thousand times smaller than observed in the convective zone of the Sun (De Jager and Versteegh, 2005). The forcing is **100 000 times smaller** than the tidal forcing of the four Gallilean satellites on Jupiter (which is similar to the tidal forcing of the Moon on Earth).
2. The ~ 11.2 years-period inferred from the ‘weak deviations from Jupiter-Venus-Earth syzygies’ is an artificial construction which has no signature in the complete tidal signal, as demonstrated by Okal and Anderson (1975), and illustrated in Appendix A.

It is therefore surprising that this idea receives a renewed attention (Scafetta, 2012; Okhlopkov, 2016; Baidolda, 2017; Courtillot, Lopes, and Le Mou el, 2021; Charbonneau, 2022). Even more surprising is the enthusiasm shown by Stefani and colleagues who have published no less than 7 articles exploiting this idea (see Stefani, Stepanov, and Weier (2021) and references therein). It seems that the main reasons that give confidence to these authors is their demonstration that the solar cycle is *clocked*, and probably the belief that this property requires a clocked forcing that only planetary motions can provide. Their demonstration, exposed in Stefani, Giesecke, and Weier (2019), rests upon the computation of ‘Dicke’s ratio’ of a 1000-years long time series of solar minima, which favors a clocked origin over a random-walk type origin.

The main objective of the present article is to show that the demonstration of Stefani, Giesecke, and Weier (2019) is invalid. I also show examples of fluid instabilities that naturally produce clocked-looking time series.

2. The demonstration of Stefani *et al* (2019)

Stefani, Giesecke, and Weier (2019) picked up an idea that Dicke (1978) proposed for testing whether there is a “*chronometer hidden deep in the Sun*”. The aim of Dicke was to distinguish a clocked behaviour from an ‘*eruption hypothesis*’, in which solar cycles would appear with a random phase. While Dicke restricted his analysis to the post-1705 time series of 25 solar maxima, Stefani, Giesecke, and Weier (2019) extend it to 92 solar cycles starting in AD 1000, in an attempt to obtain a better statistical significance.

2.1. Dicke’s ratio

Dicke (1978) noticed that a succession of 3 very short cycles starting in 1755 was followed by a very long cycle, as if the Sun was trying to keep up with some

²alignment of all these planets with the Sun.

internal clock. He proposed several statistical tools to assess the existence of such a clock.

Consider a time series $t(i)$ of N events i . In a perfectly clocked time series, all event dates $t(i)$ are evenly spaced. When gaussian distributed noise is added, each event date is displaced from the regular grid by some random time, yielding a corresponding distribution of cycle durations $d(i) = t(i) - t(i-1)$. In contrast, when events occur with a random phase, cycle durations $d(i)$ have a gaussian distribution, and event dates are obtained as $t(i) = t(i-1) + d(i)$. Clocked and random-walk time series can yield the same mean cycle duration \bar{d} and standard deviation σ , but their statistical properties are not all identical.

Dicke (1978) introduced a ratio that measures this difference, which Stefani, Giesecke, and Weier (2019) refer to as ‘Dicke’s ratio’. Dicke’s ratio $Di(n)$ computed for subsets of $n \leq N$ consecutive events is defined by:

$$Di(n) = \frac{\sum_{i=2}^n \delta_n^2(i)}{\sum_{i=2}^n (\delta_n(i) - \delta_n(i-1))^2}, \quad (1)$$

where $\delta_n(i) = t(i) - f_n(i)$ is the deviation of event date $t(i)$ from a best linear fit $f_n(i) = a_n i + b_n$ of the n dates.

According to Dicke (1978), the expectation of Dicke’s ratio is:

$$\mathbb{E}(Di_{clock}(n)) = \frac{n^2 - 1}{2(n^2 + 2n + 3)} \rightarrow \frac{1}{2} \text{ when } n \rightarrow \infty \quad (2)$$

for a clocked time series, while it is:

$$\mathbb{E}(Di_{rand}(n)) = \frac{(n+2)(n^2-1)}{3(5n^2+6n-3)} \rightarrow \frac{1}{15}n \text{ when } n \rightarrow \infty \quad (3)$$

for a random-walk time series.

The expectation of $Di(n)$ is independent of \bar{d} and σ for both families, but the spread around the expectation does depend upon σ . Dicke (1978) applied this statistical tool to the time series of sunspot numbers starting in 1705. Due to the limited number of cycles, he could not reach a very definitive conclusion.

2.2. Schove’s solar cycle time series

To reach a firmer conclusion, Stefani, Giesecke, and Weier (2019) complemented the post-1705 solar minima series by solar minima dates as far back as AD 1000, following Schove (1955). Indeed, Schove published in 1955 the outcome of a very ambitious venture: dating maxima and minima of the solar cycle from 653 BC to AD 2025! Pre-1705 observations of sunspots being very rare, he mostly relied on reports of the observation of polar aurorae. In order to make up for the limited amount of reliable data, Schove (1955) explicitly mentions (p.131) that he made use of two **assumptions** to build his 26-century-long table. These assumptions are reproduced in Figure 1.

-
- (a) **The time between successive maxima was never less than 8 and never more than 16 years.**
 (b) **There are 9 maxima in 100 years.**

Figure 1. The two assumptions made by Schove (1955) to construct his series of solar maxima, as displayed in his article p.131.

3. Arguments for a rebuttal

Schove's assumption (b) as listed in Figure 1 clearly suggests that his time series of solar maxima is **clocked by construction**. In order to be more specific, I have built synthetic solar cycles to test the impact of Schove's assumptions on the character of the resulting time series.

3.1. Synthetic solar cycles

The well-documented 24 solar cycles from 1755 yield a cycle duration (time between maxima) of 11.0 ± 2.0 years. Extending backwards to AD 1000 with Schove's dates yields 92 maxima separated by 11.1 ± 2.2 years. I have built two different families of synthetic cycles: a random-walk family, and a clocked family. Both retain the post-1755 dates of solar maxima, as distributed by WDC-SILSO, Royal Observatory of Belgium, Brussels (SILSO World Data Center, 1755–2019).

- The random-walk series are built by drawing at random normally distributed cycle durations, with a mean of 11.1 years and a standard deviation of 2.0 years. The dates of maxima are then constructed by cumulative difference from the date of the oldest post-1755 maximum.
- The clocked series are built by extending the post-1755 dates of maxima backwards in time with a constant duration of 11.1 years, and then adding to the obtained dates a normal random noise with zero-mean and a standard deviation of 1.5 years, this value providing the desired standard deviation of 2.0 years for cycle durations.

Figure 2 displays the probability density function (pdf) obtained with 10 000 realizations, for both the random-walk series (Figure 2a) and the clocked series (Figure 2b). The pdf of Schove series is also drawn in Figure 2b.

3.2. The impact of Schove's assumptions

I have examined which of the 10 000 realizations of both families comply with the two assumptions of Schove (1955) recalled in Figure 1. I find only 3 random-walk realizations, and 42 clocked realizations. In other words, the **assumptions** used by Schove (1955) practically exclude random variations of the duration between solar maxima.

The cycle duration pdf of Schove-compliant realizations are shown in Figure 2, while their time series and deviations from a linear fit are displayed in Appendix B together with those of Schove's series.

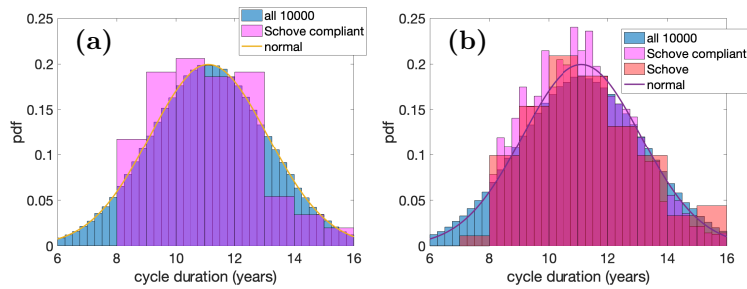


Figure 2. Probability density function of the duration of synthetic solar cycles. (a) Random-walk synthetics: gaussian distribution of all 10 000 realizations (teal), and pdf of the 3 realizations that comply with Schove’s assumptions (magenta). (b) Clocked synthetics: nearly gaussian distribution of the 10 000 realizations (teal), pdf of the 42 Schove-compliant realizations (magenta), and pdf of Schove cycle durations (red).

Figure 3 shows Dicke’s ratios³ for a random selection of 100 realizations of both families. The thick black line shows the mean of Dicke’s ratio for all realizations, while the thick red line is the mean of the Schove-compliant realizations. Note that Dicke’s ratio of the rare Schove-compliant random-walk series is much lower than the mean of all realizations, and that individual realizations can plot far from the mean.

4. Quasi-clocked magnetohydrodynamic instabilities

The original goal of Dicke (1978) was to test the compatibility of solar cycle time series with an ‘eruption hypothesis’ expressed by Kiepenheuer (1959) as ‘each cycle represents an independent eruption of the Sun which takes about 11 years to die down’. Fluid dynamics and magnetohydrodynamics instabilities do not necessarily behave that way, even when strong turbulence is present. For example, quasi-periodic magnetic oscillations have been reported in the VKS dynamo experiment (Berhanu et al., 2009) at Reynolds numbers above 10^7 . Nonetheless, we have seen that Dicke’s ratio yields a more stringent measure of the clocked behaviour of a time series than provided by visual inspection or pdf.

The Grenoble DTSΩ liquid sodium experiment exhibits magnetic fluctuations that are often quite regular (Schmitt et al., 2008). From one such experiment, I have extracted time series of maximum induced magnetic intensity (see Appendix C for details), and computed Dicke’s ratio of several sequences of 100 consecutive maxima. Figure 4 shows that the behaviour of these magnetic fluctuations is quasi-clocked, even though the Reynolds number is $\simeq 8 \times 10^6$ and the standard deviation of the fluctuations about 30%.

³Note that all Dicke’s ratios are calculated backwards in time as in Stefani, Giesecke, and Weier (2019), since more recent dates are considered more reliable.

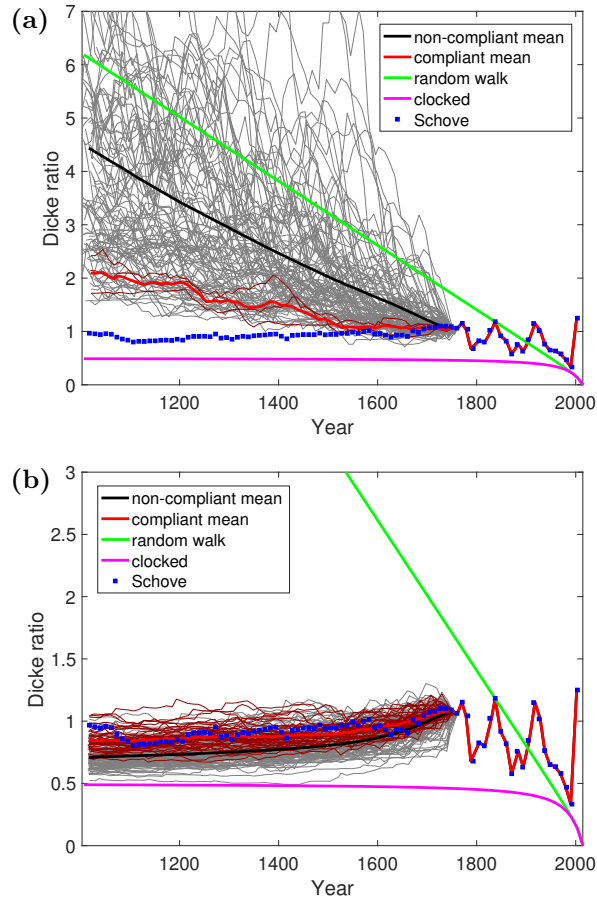


Figure 3. Dicke's ratios of (a) random-walk and (b) clocked synthetic solar cycles. Random selection of 100 realizations (grey), mean of all 10 000 realizations (thick black), Schove-compliant realizations (red) and their mean (thick red), Schove time series (blue squares). The thick green and magenta lines show the expectation of Dicke's ratio for a random-walk (equation 3) and for a clocked law (equation 2), respectively. Note that all synthetics share the same post-1755 reliable time series.

5. Conclusion

The demonstration by Stefani, Giesecke, and Weier (2019) of a clocked behaviour for solar cycles is invalid because the 1000 years long time series they use (Schove, 1955) is **clocked by construction**. The astrological quest for a link between solar cycles and planetary tides remains as unfounded as ever. Magnetohydrodynamics instabilities can produce quasi-periodic fluctuations that appear as almost clocked.

Acknowledgments I thank André Giesecke and Frank Stefani for providing clarifications on their computation of Dicke's ratio. I thank my colleagues of the geodynamo team of ISTERre for useful discussions and encouragements, and an anonymous reviewer for helpful suggestions. This article is dedicated to Emile Okal and to the memory of Don L. Anderson.

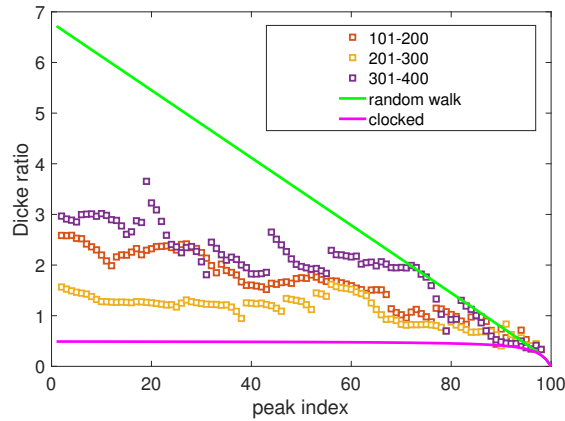


Figure 4. Dicke’s ratio of magnetic fluctuations in the DTSΩ liquid sodium experiment (see Appendix C for details). Three consecutive series of 100 maxima are plotted (peaks 101 to 200, 201 to 300, and 301 to 400). The green and magenta lines show the expectation of Dicke’s ratio for a random-walk (equation 3) and for a clocked law (equation 2), respectively.

Materials Availability All matlab scripts and data used to produce the figures of this article are available as supplementary material.

Conflict of interest The author declares that he has no conflicts of interest.

Appendix

A. Frequency spectra of synthetic tidal forcings

I have built synthetic tidal forcings to illustrate the lack of evidence for a 11.2 years periodicity, as demonstrated by Okal and Anderson (1975). I model the tidal forcing exerted by Jupiter, Venus, Earth and Mercury, assuming circular orbits, and starting at a time when all planets are aligned. Mass, distances and orbital periods are taken from <https://nssdc.gsfc.nasa.gov/planetary/factsheet/>.

Tidal forcing of this simplified planetary system at a given meridian on the Sun can be expressed as:

$$Tide(t) = \sum_p \frac{m_p}{d_p^3} \left[\cos^2 \left(2\pi \frac{t}{T_S} - 2\pi \frac{t}{T_p} \right) - \frac{1}{3} \right], \quad (4)$$

where m_p and d_p are the mass and distance from the Sun of planet p , respectively. T_p is its orbital period, while T_S is the duration of a solar day, taken as 27 days.

Figure 5a shows the predicted tidal signal over a period of 10 000 days (27.4 years). The orbital period of Jupiter (11.86 years) is indicated by vertical red bars. The maximum tidal forcing achieved at $t = 0$ is marked by a horizontal dashed line. It can be seen that forcings almost as large occur many times during one orbital period of Jupiter, typically each time Jupiter and Venus are aligned with the Sun.

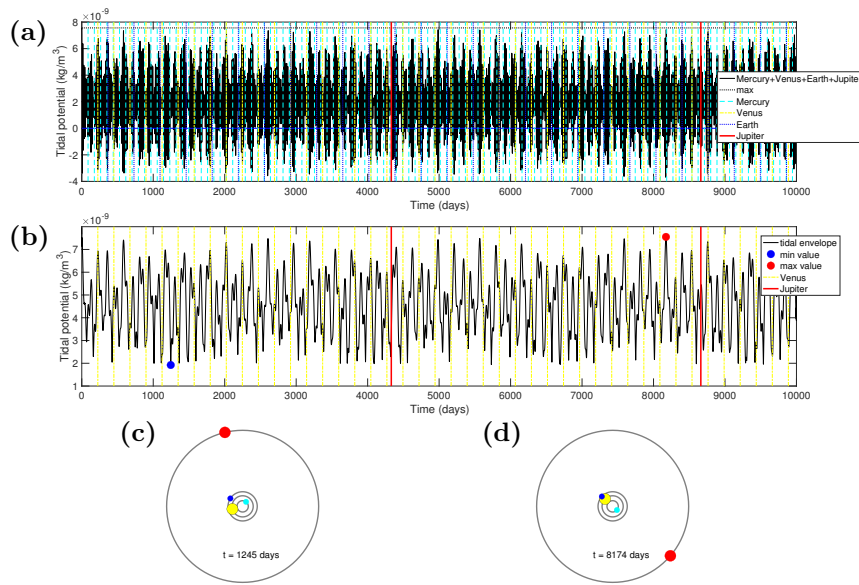


Figure 5. Time series and envelope of tidal forcing as a function of time in a realistic synthetic solar system. (a) Tidal forcing at a given meridian on the Sun, calculated from equation 4 over 10 000 days (27.4 years). The periods of the 4 planets are marked by vertical lines of different colors. The maximum tide (achieved at $t = 0$) is shown by a horizontal dashed black line. (b) envelope of the tidal forcing. The minimum and (second) maximum are marked by a blue dot and a red dot, respectively. The periods of Jupiter and Venus are shown by vertical lines. (c) Positions of the 4 planets at the minimum tide ($t = 1245$ days). (d) Positions of the 4 planets at the (second) maximum tide ($t = 8174$ days).

Tidal minima are better seen in Figure 5b, which displays the envelope of the tidal signal. The minimum of the series (at $t = 1245$ days) is marked by a blue dot, while the second maximum (at $t = 8174$ days) is shown by a red dot. The corresponding positions of the 4 planets are given in Figures 5c and 5d; respectively. As expected, all 4 planets are almost aligned with the Sun at the maximum, while Jupiter cancels Venus' tide and Mercury cancels the Earth's tide at the minimum.

Figure 6 presents the spectra of a 360 years-long synthetic tidal signal (blue) and of its envelope (orange). The 4 peaks of the former simply correspond to half a solar day as seen from each planet (see equation 4). The spectrum of the envelope is dominated by peaks at the periods of syzygies of pairs of planets with the Sun, and their overtones. The spectrum is almost flat for periods beyond 300 days. This plot mimics Figure 3 of Okal and Anderson (1975), which shows the full tidal spectrum, ‘taking into account the complete orbital elements [of the 4 planets], including eccentricity, inclination and their variation with time’ over a period of 1 800 years. Orbital eccentricity adds up small tidal peaks at the orbital periods of Jupiter (11.86 years) and Mercury (0.241 years), but nothing shows up at 11.2 years (4088 days), as emphasized by Okal and Anderson (1975).

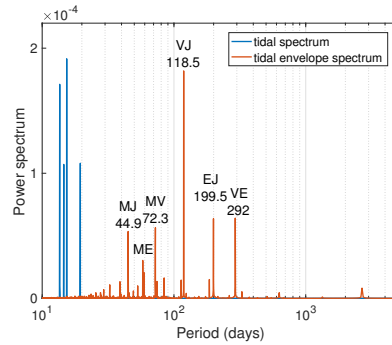


Figure 6. Power spectra of the tidal signal (blue) and of its envelope (orange), as a function of period. Tidal peaks of the envelope spectrum appear at syzygies of pairs of planets with the Sun. Following Okal and Anderson (1975), I label them with the initials of the two planets. The largest tide is ‘VJ’ at 118.5 days when Venus and Jupiter are aligned with the Sun.

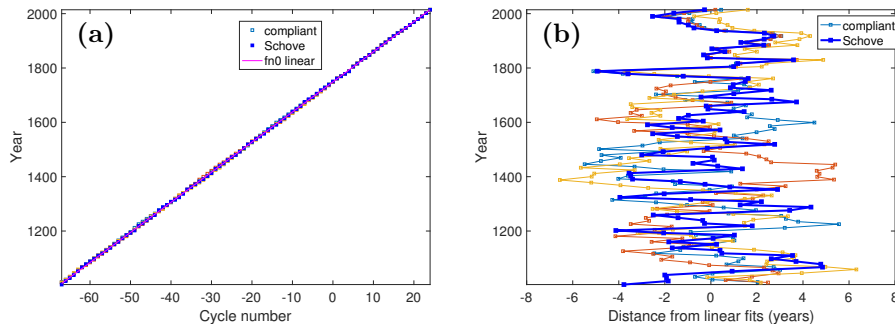


Figure 7. (a) Time series and (b) deviations of Schove-compliant random-walk synthetic solar cycles. The blue squares are for Schove’s maxima before 1755, and from SILSO World Data Center (1755–2019) after 1755.

B. Time series and deviations of synthetic solar maxima

Figures 7 and 8 display the time series and deviations of the synthetic solar cycles that comply with Schove’s assumptions, to compare with Figure 1 of Stefani, Giesecke, and Weier (2019). Deviations of each realization are the difference between dates of maxima and a linear fit of these dates.

C. Dicke’s ratio of magnetic fluctuations in the $DTS\Omega$ experiment

The $DTS\Omega$ experiment was built to study magnetohydrodynamics in the magnetostrophic regime, in which Lorentz and Coriolis forces are dominant. Fifty liters of liquid sodium are enclosed in a spherical container that can rotate around a vertical axis. An inner central sphere can rotate independently around the same axis, and hosts a strong permanent magnet producing an axial dipolar magnetic

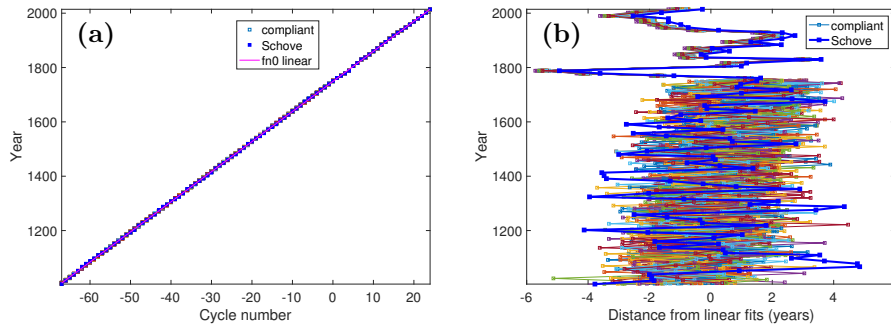


Figure 8. (a) Time series and (b) deviations of Schove-compliant clocked synthetic solar cycles. The blue squares are for Schove’s maxima before 1755, and from SILSO World Data Center (1755–2019) after 1755.

field. The 3 components of the induced magnetic field are measured at the surface of the outer sphere at 20 equally-spaced latitudes from -57° to 57° (see Schmitt et al. (2013) for more details). The frequency spectra of electric and magnetic fluctuations reveal a quasi-periodic behaviour that can be linked to the presence of magneto-Coriolis waves (Schmitt et al., 2008, 2013) or instabilities (Figueroa et al., 2013; Kaplan, Nataf, and Schaeffer, 2018).

An example of such quasi-periodic magnetic fluctuations is given in Figure 9. The spin rate of the outer sphere is $f_o \simeq 10$ Hz, while the differential rotation of the inner sphere is $\Delta f \simeq -20$ Hz, yielding fluid velocities $U \simeq 25$ m/s. With an outer radius $r_o = 0.21$ m, the Reynolds number $Re = \frac{U r_o}{\nu} \simeq 8 \times 10^6$ and the magnetic Reynolds number $Rm = \frac{U r_o}{\eta} \simeq 60$, with ν the kinematic viscosity, and η the magnetic diffusivity. Figure 9a displays a latitude-versus-time color-coded image of the squared azimuthal magnetic fluctuations averaged over one turn of the inner sphere, in a time-window of some 250 rotations of the inner sphere. Latitudinally-coherent quasi-periodic fluctuations of variable intensity dominate. Figure 9b is the time-record of the same fluctuations at a latitude of 9° . I have extracted the 100 maxima of this record, plotted as triangles in figure 9b. The duration between maxima is 0.11 ± 0.03 s. Dicke’s ratio of the resulting time series is plotted in Figure 4, together with Dicke’s ratio of the previous and next series of 100 maxima. All three series appear to be closer to a ‘clocked’ behaviour than to a random-walk behaviour.

References

- Baidolda, F.: 2017, Search for planetary influences on solar activity. PhD thesis, Université Paris sciences et lettres.
- Berhanu, M., Gallet, B., Monchaux, R., Bourgoïn, M., Odier, P., Pinton, J.-F., Plihon, N., Volk, R., Fauve, S., Mordant, N., et al.: 2009, Bistability between a stationary and an oscillatory dynamo in a turbulent flow of liquid sodium. *Journal of Fluid Mechanics* **641**, 217.
- Charbonneau, P.: 2022, External Forcing of the Solar Dynamo. *Frontiers in Astronomy and Space Sciences* **9**, 853676.

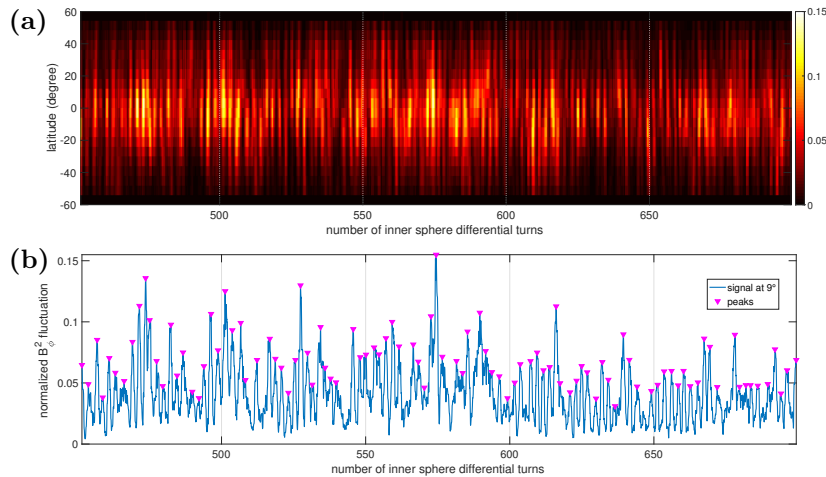


Figure 9. Magnetic fluctuations in the $DTS\Omega$ experiment. (a) Color-coded image of the square of azimuthal magnetic field fluctuations, normalized by the square of the imposed magnetic field (%) at the surface of the outer sphere. The magnetic field is measured at the 20 latitudes which form the y-axis. The x-axis is time given in number of turns of the inner sphere with respect to the outer sphere. The records are averaged over one such differential turn. (b) Extraction of the same signals at a latitude of 9° , showing a succession of peaks labelled by magenta triangles.

- Courtillet, V., Lopes, F., Le Mouél, J.: 2021, On the prediction of solar cycles. *Solar Physics* **296**, 1.
- De Jager, C., Versteegh, G.J.: 2005, Do planetary motions drive solar variability? *Solar Physics* **229**, 175.
- Dicke, R.: 1978, Is there a chronometer hidden deep in the Sun? *Nature* **276**, 676.
- Figueroa, A., Schaeffer, N., Nataf, H.-C., Schmitt, D.: 2013, Modes and instabilities in magnetized spherical Couette flow. *Journal of Fluid Mechanics* **716**, 445.
- Kaplan, E., Nataf, H.-C., Schaeffer, N.: 2018, Dynamic domains of the Derviche Tourneur sodium experiment: Simulations of a spherical magnetized Couette flow. *Physical Review Fluids* **3**, 034608.
- Kiepenheuer, K.: 1959, *The Sun*, University of Michigan Press.
- Malburet, J.: 1918, *Sur la période des maxima d'activité solaire*, Pli cacheté 8539, Acad. Sci. Paris.
- Malburet, J.: 1925, Sur la cause de la périodicité des tâches solaires. *L'Astronomie* **39**, 503.
- Malburet, J.: 2019, Sur la période des maxima d'activité solaire. *Comptes Rendus Geoscience* **351**, 351.
- Okal, E., Anderson, D.L.: 1975, On the planetary theory of sunspots. *Nature* **253**, 511.
- Okhlopov, V.: 2016, The gravitational influence of Venus, the Earth, and Jupiter on the 11-year cycle of solar activity. *Moscow University Physics Bulletin* **71**, 440.
- Scafetta, N.: 2012, Does the Sun work as a nuclear fusion amplifier of planetary tidal forcing? A proposal for a physical mechanism based on the mass-luminosity relation. *Journal of Atmospheric and Solar-Terrestrial Physics* **81**, 27.
- Schmitt, D., Alboussière, T., Brito, D., Cardin, P., Gagnière, N., Jault, D., Nataf, H.-C.: 2008, Rotating spherical Couette flow in a dipolar magnetic field : Experimental study of magneto-inertial waves. *J. Fluid Mech.* **604**, 175.
- Schmitt, D., Cardin, P., La Rizza, P., Nataf, H.-C.: 2013, Magneto-Coriolis waves in a spherical Couette flow experiment. *European J. Mech. B/Fluids* **37**, 10.
- Schove, D.J.: 1955, The sunspot cycle, 649 BC to AD 2000. *Journal of Geophysical Research* **60**, 127.
- SILSO World Data Center: 1755–2019, The International Sunspot Number. *International Sunspot Number Monthly Bulletin and online catalogue*. [ADS](#).

- Stefani, F., Giesecke, A., Weier, T.: 2019, A model of a tidally synchronized solar dynamo. *Solar Physics* **294**, 1.
- Stefani, F., Stepanov, R., Weier, T.: 2021, Shaken and Stirred: When Bond Meets Suess–de Vries and Gnevyshev–Ohl. *Solar Physics* **296**, 1.
- Wood, K.: 1972, Physical sciences: sunspots and planets. *Nature* **240**, 91.